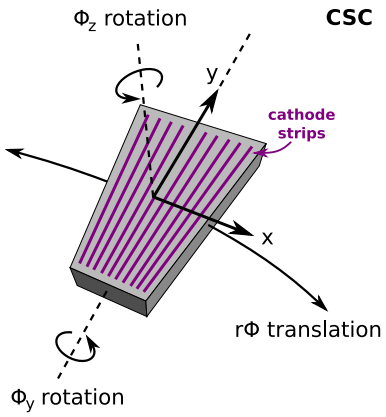

Figure 1: Schematic CSC chamber, indicating the local coordinate system.

1 Introduction

The muon endcap was aligned using information from four different sources: photogrammetry, the Muon Endcap Alignment System, tracks from beam-halo muons, and tracks from collisions muons. Some of these sources of information are orthogonal, while others provide for cross-checks between the different systems. To combine information, alignment corrections were applied in a well-defined sequence, such that each step benefits from the previous. Potentially interdependent corrections were iterated to obtain a mutually consistent solution.

2 Measurement of disk bending with the Muon Endcap Alignment System

3 Internal-ring alignment using beam-halo tracks

CSC chambers overlap slightly along their edges, and muons passing through these narrow regions provide information about the relative displacement of the neighboring chambers. To produce a complete geometry from the pairwise chamber information, the following objective function is minimized:

$$\chi^2 = \sum_{m_{ij}}^{\text{constraints}} \frac{(m_{ij} - A_i + A_j)^2}{{\sigma_{ij}}^2} + \lambda \left(\frac{1}{N_{\text{chambers}}} \sum_{i}^{\text{chambers}} A_i \right)^2 \quad (1)$$

where A_i are the chamber coordinates to optimize, $m_{ij} \pm \sigma_{ij}$ are the pairwise chamber measurements, and λ is a Lagrange multiplier to constrain the floating coordinate system. Two types of constraints are used: beam-halo tracks and photogrammetry measurements, with the latter applied only to pairs of chambers that were missing track data due to inefficient read-out electronics (14 out of 396 pairs of neighboring chambers). The alignment proceeds in alternating passes, first aligning $r\phi$ positions (A_i are interpreted as positions and m_{ij} are

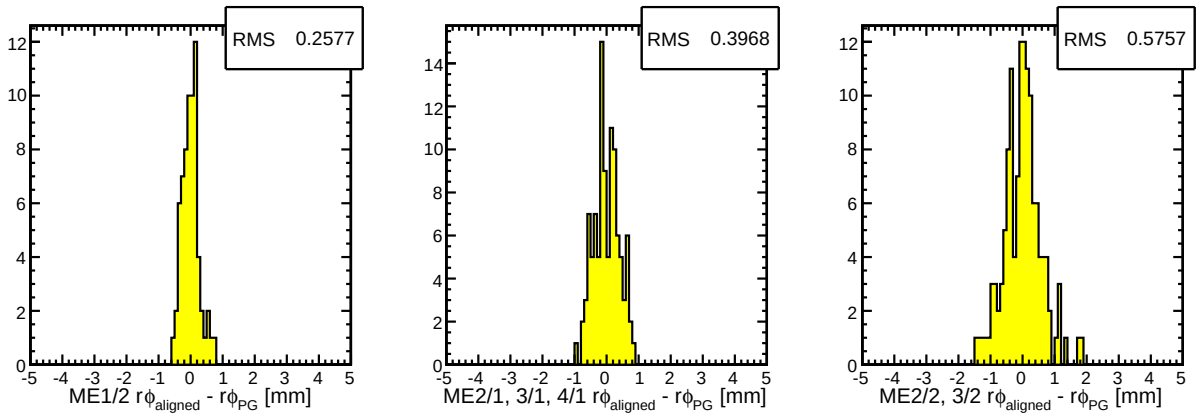

Figure 2: Chamber positions after internal-ring alignment compared with photogrammetry, split by ring. (ME1/1 chambers were not measured by the photogrammetry.)

residuals), then ϕ_z angles (A_i are chamber angles and m_{ij} are residuals-times-lever arm). The alignment fully converged after one $r\phi$ pass and one ϕ_z pass.

Although photogrammetry information was used to constrain a fraction of the chambers, much larger weights were given to the beam-halo data, in inverse proportion to the square of the measurement uncertainties in the two methods. As seen in Fig. 2, the level of agreement between the track-based technique and photogrammetry is 0.3–0.6 mm. This is much smaller than the typical scale of chamber corrections from design geometry (2–3 mm).

4 Whole-ring placement using collisions muons

To complete the endcap alignment, the internally aligned rings must be aligned relative to one another and the tracker. Tracks from the tracker were propagated to the muon chambers and whole-ring corrections were derived from the pattern of $r\phi$ residuals as a function of global ϕ. A constant offset in the residuals is interpreted as a rotation of the ring in ϕ_z, while terms proportional to $\cos\phi$ and $\sin\phi$ are interpreted as displacements in global x and y, respectively.

Figure 3 provides an example of an alignment fit for one ring (ME$-$2/1). The alignment was performed in one pass, with a second to verify self-consistency.

To cross-check the alignment using a qualitatively different method, beam-halo tracks crossing an entire endcap (three or four stations, depending on distance from the beamline) were used to calculate residuals in one station relative to segments in another. Figure 4 shows an example, in which ME+3/1 segments were propagated linearly (no corrections for material or magnetic field) to ME+4/1. These plots were not used to perform the alignment, so the fact that the strong ϕ trend observed before alignment is eliminated in the aligned geometry adds confidence to the result.

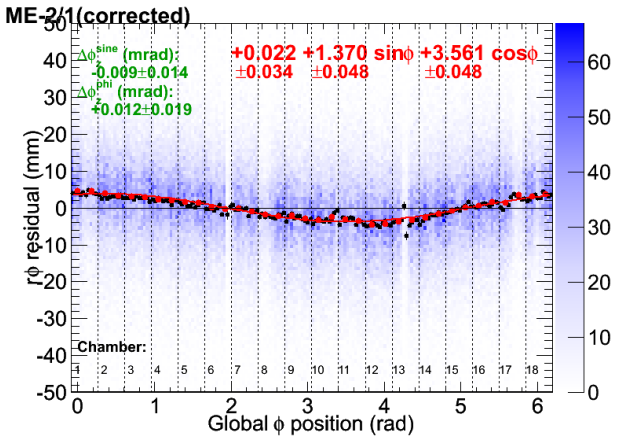

Figure 3: Residuals plot used to align a ring: the color scale is the residuals distribution versus ϕ, black points are a profile derived from truncated-Gaussian peak fits in each ϕ bin, and red points are the average of peak-fits to muons and antimuons separately. The fitted curve is interpreted as three alignment degrees of freedom. Vertical dashed lines indicate the boundaries between chambers.

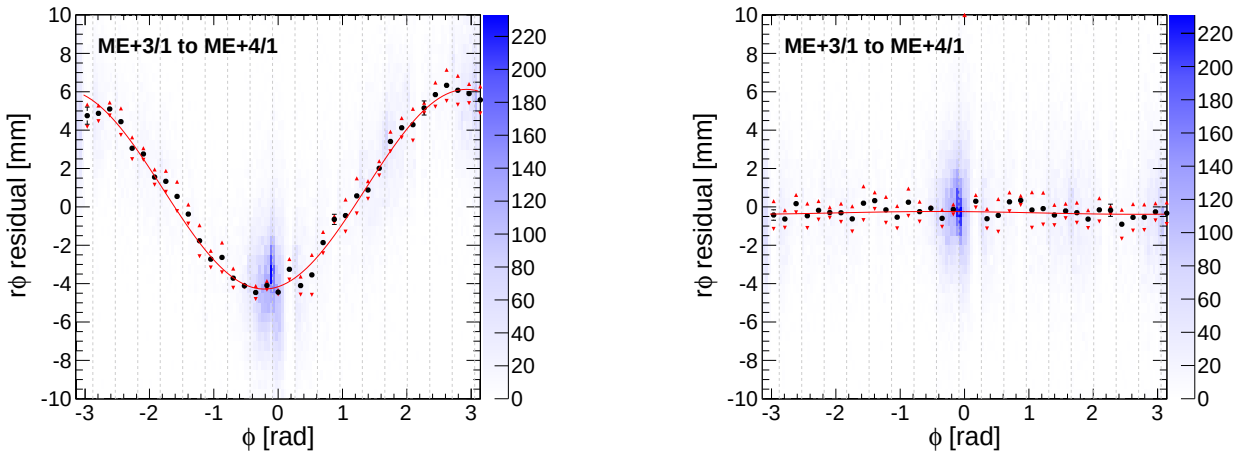

Figure 4: Residuals from beam-halo tracks used to cross-check the alignment performed with collisions. The symbols in these plots have the same meaning as Fig. 3, though residuals were calculated differently (see text). Left: before alignment. Right: after alignment using collisions (not beam-halo).